frontiers | Frontiers in Marine Science

TYPE Original Research
PUBLISHED 20 July 2023
DOI 10.3389/fmars.2023.1222157

OPEN ACCESS

EDITED BY
Danny Ionescu,
Leibniz-Institute of Freshwater Ecology and Inland Fisheries (IGB), Germany

REVIEWED BY
Jiwen Liu,
Ocean University of China, China
Wei Li,
Shantou University, China

*CORRESPONDENCE
Xue-Wei Xu
xuxw@sio.org.cn
Cong Sun
michael_sc@sina.com

RECEIVED 13 May 2023
ACCEPTED 03 July 2023
PUBLISHED 20 July 2023

CITATION
Ma K-J, Ye Y-L, Fu Y-H, Fu G-Y, Sun C and Xu X-W (2023) Genomic and phylotypic properties of three novel marine *Bacteroidota* from bare tidal flats reveal insights into their potential of polysaccharide metabolism.
Front. Mar. Sci. 10:1222157.
doi: 10.3389/fmars.2023.1222157

Genomic and phylotypic properties of three novel marine *Bacteroidota* from bare tidal flats reveal insights into their potential of polysaccharide metabolism

Kuo-Jian Ma[1,2], Yong-Lian Ye[1], Yun-Han Fu[1,2], Ge-Yi Fu[1], Cong Sun[3,4]* and Xue-Wei Xu[1,2]*

[1]Key Laboratory of Marine Ecosystem Dynamics, Ministry of Natural Resources and Second Institute of Oceanography, Ministry of Natural Resources, Hangzhou, China, [2]Ocean College, Zhejiang University, Zhoushan, China, [3]College of Life Sciences and Medicine, Zhejiang Sci-Tech University, Hangzhou, China, [4]Center of Marine Microbial Resource, Zhejiang Sci-Tech University Shaoxing Academy of Biomedicine Co., Ltd., Shaoxing, China

Special geographical location and abundant organic matter profiles in tidal flats have resulted in great microbial diversity, in which *Bacteroidota* strains are considered as one of the primary degraders of polysaccharides, playing a crucial role in the carbon cycle. In this study, we collected sediment or sand samples from 34 bare tidal flats in China and investigated the profile of culturable bacteria, selected three *Bacteroidota* for polyphasic taxonomic analysis and revealed their polysaccharide metabolic potential. Totally, we isolated 352 pure cultured bacteria and they mainly distributed in *Bacteroidota*, *Pseudomonadota*, *Bacillota*, and *Actinomycetota*. It is shown that the bare tidal flats contained a large number of potential novel species, mainly distributed in *Flavobacteriales* and *Cytophagales* within *Bacteroidota*. Three *Bacteroidota* strains, M17^T, M82^T, and M415^T, isolated from mudflat were selected for polyphasic taxonomic analysis. The 16S rRNA gene sequence similarity between strain M17^T and *Mangrovivirga cuniculi* KCTC 72349^T was 99.28%, and less than 90.09% with other species; strain M82^T shared the highest 16S rRNA gene sequence similarity of 97.85% with *Pontibacter litorisediminis* KCTC 52252^T, and less than 97.43% with other species; strain M415T had higher 16S rRNA gene sequence similarities with type species of genera *Eudoraea* (92.62-93.68%), *Zeaxanthinibacter* (92.02-92.91%), and *Muriicola* (92.21-92.83%). Phylogenetic analysis based on 16S rRNA gene sequences and single-copy orthologous clusters showed that strains M17^T and M82^T represent novel species within the genus *Mangrovivirga* and *Pontibacter*, respectively, and strain M415^T represents a novel species of a novel genus within the family *Flavobacteriaceae*. The potential in polysaccharide metabolism of all these three strains was analyzed by genomes. The analysis revealed that glycoside hydrolases and glycosyltransferases account for more than 70% of the total CAZymes.

Additionally, the numbers of polysaccharide utilization loci (PULs) and annotated CAZymes in *Cytophagales* spp. M17^T and M82^T were found to be higher than those in *Flavobacteriales* sp. M415^T. Highly specialized saccharolytic systems and the presence of numerous diversified CAZymes for obtaining energy through polysaccharide metabolism were speculated to help the three novel strains adapt to the utilization of both terrestrial and marine polysaccharides.

KEYWORDS

bare tidal flats, culturable bacteria, CAZymes, polysaccharide utilization loci, bacteroidota

1 Introduction

Tidal flats are located in the intertidal zone between the high- and low-tide levels (Murray et al., 2019; Wang et al., 2020b). Recent research showed that tidal flats occupy at least 127,921 km^2 globally, mainly distributed along the coast of Asia, especially China (Murray et al., 2019). Due to their unique geographical location and periodic changes in environmental factors such as salinity, temperature, dissolved oxygen, light intensity, tides, ocean currents, and human disturbance, tidal flats have become one of the most productive and vulnerable environments in the world (Underwood and Kromkamp, 1999; Mayor et al., 2018; Chang et al., 2022). At the same time, tidal flats play important roles in carbon sequestration (Howard et al., 2014; Sasmito et al., 2020), aquaculture (Ni et al., 2020), microbial diversity, and function research (Mayor et al., 2018; Perillo et al., 2018). Lots of studies mainly focused on the special vegetated tidal flats such as mangrove and salt marsh; however, the studies on bare tidal flats (also referred to unvegetated tidal flats) were relatively limited.

With the rapid development of high-throughput sequencing technologies, our understanding of microbial diversity, structure, and function in bare tidal flats has tremendously expanded in recent years (Gong et al., 2019; Zhang et al., 2021; Rinke et al., 2022). Microbial diversity in mudflats is extremely high and significantly varies with different substrates and depths, playing an essential role in organic matter catabolism and even carbon fixation (Molari et al., 2012; Choi et al., 2018; Gaubert-Boussarie et al., 2020; Mohapatra et al., 2021). The degradation and metabolism process involved by bacteria and archaea in bare tidal flats is an important part of the global cycle of carbon, nitrogen, phosphorus, sulfur, and other elements (Ettwig et al., 2010; Bauer et al., 2013), which has a profound impact on the content of atmospheric greenhouse gases and the rate of element cycling.

Although the well-known hypothesis said "only 1% of microbes are culturable" (Amann et al., 1995; Torsvik and Ovreas, 2002), more and more scientists believe that more than 1% of microbes can be culturable (Martiny, 2019; Steen et al., 2019). High-throughput sequencing technologies provide a comprehensive understanding of microbial diversity; pure culture of microorganisms is also of great importance, which can help us to elucidate the physiological mechanism and ecological function of microorganisms, as well as find new metabolic pathways and metabolites (Guo et al., 2006), such as *Bacteroidota* strains which play important roles in polysaccharide degradation, which account for roughly 75% of the annually renewable biomass (Lichtenthaler and Peters, 2004; Lapebie et al., 2019; Gavriilidou et al., 2020; McKee et al., 2021).

Marine representatives of the phylum *Bacteroidota* possess diverse enzyme repertoires and flexible polysaccharide metabolism, actively participating in numerous biogeochemical processes (Fernández-Gómez et al., 2013). Highly specialized bacterial strains of the phylum *Bacteroidota* exhibit prolific proliferation during phytoplankton blooms and serve as primary degraders of microalgal polysaccharides (Unfried et al., 2018). In phylum *Bacteroidota*, members of the family *Flavobacteriaceae* exhibit a high proportion and diversity of carbohydrate-active enzymes (CAZymes) within their polysaccharide utilization loci (PULs), which supports their ability to utilize a wide range of polysaccharides (Kappelmann et al., 2019). For instance, *Zobellia galactanivorans* Dsij^T has emerged as a model organism for studying polysaccharide degradation in marine flavobacteria (Barbeyron et al., 2016), *Z. amurskyensis* KMM 3526^T and *Z. laminariae* KMM 3676^T possess a relatively high proportion of CAZymes (accounting for 6.49% and 5.93% of all predicted coding sequences, respectively) and are specialized in the degradation of algal polysaccharides (Chernysheva et al., 2019). In this study, we investigated the culturable bacterial proportion in the sediments from 34 sampling stations of bare tidal flats, selected three novel *Bacteroidota* strains for polyphasic taxonomy, and further analyzed their potential in polysaccharide metabolism.

2 Materials and methods

2.1 Sample collection and strain isolation

All samples were collected by a self-made cylindrical plexiglass tube sampler, transferred into sterile sample tubes after being fully homogenized, stored in a 4°C–6°C incubator, and transported to the laboratory as soon as possible. The distribution of samples is presented in Figure 1. The particle size of the sediments was determined using a laser particle size analyzer, and the sediment types were classified according to the modification of Folk's

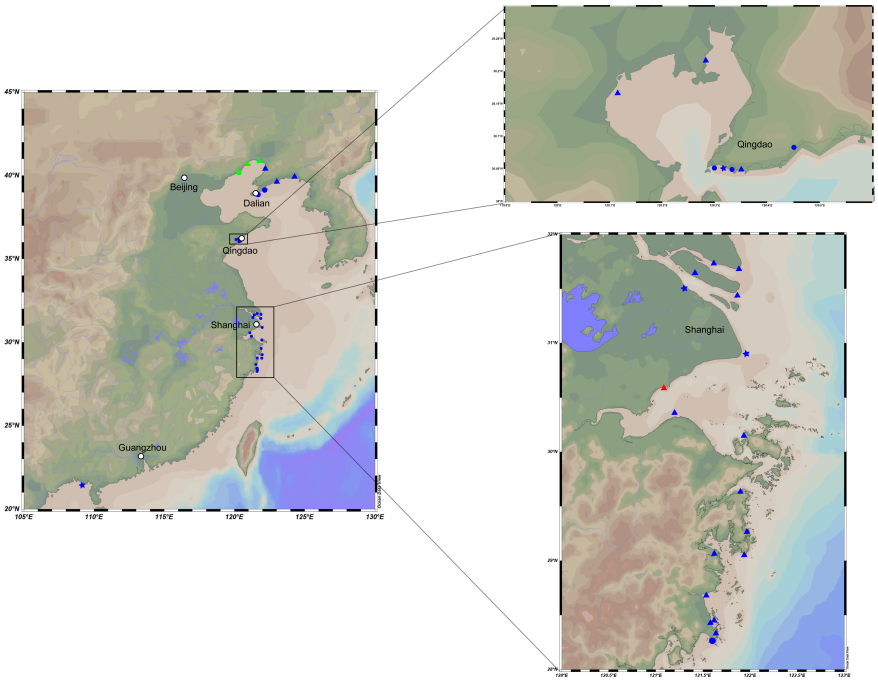

FIGURE 1
Map representing locations of the intertidal sediment sampling stations. Dots in these plots represent different substrate types and sample depths. Triangle, mud flat; circle, sand flat; star, muddy sand flat. Blue, 0–5-cm depth; red, 5–15-cm depth; green, 15–25-cm depth.

classification of sediments: sand (greater than 10% of particles with a diameter less than 63 μm), muddy sand (10%–90% of particles with a diameter less than 63 μm), and mud (less than 10% of particles with a diameter less than 63 μm) (Folk et al., 1970). Strain M17^T was isolated from an intertidal mudflat (0–5 cm) collected from Qingdao, Shandong Provence (36°10′ N, 120°07′ E); strains M82^T and M415^T were isolated from two intertidal mudflats (0–5 cm) collected from Taizhou, Zhejiang Provence (28°27′ N, 121°37′ E and 29°4′ N, 121°37′ E, respectively).

Samples were serially diluted to 10^{-3} with sterile seawater using the standard dilution-plating method (Williams and Davies, 1965). Generally, a 100-μL aliquot of each dilution was spread on modified marine agar (per liter of distilled water: Bacto yeast extract 0.1 g, Bacto peptone 0.5 g, ferric citrate 0.1 g, NaCl 19.45 g, $MgCl_2{\cdot}6H_2O$ 12.6 g, $MgSO_4$ 3.24 g, $CaCl_2$ 1.8 g, KCl 0.55 g, $NaHCO_3$ 0.16 g, KBr 0.08 g, $SrCl_2$ 34.0 mg, $NaSiO_3$ 4.0 mg, NH_4NO_3 1.6 mg, H_3BO_4 22.0 mg, NaF 2.4 mg, Na_2HPO_4 8.0 mg, agar 20 g) and incubated at 30°C for 3–7 days to a simulated oligotrophic environment. Afterward, the strains were isolated from different plates and purified by repeating streaking. All bacterial cultures were stored in Marine Broth 2216 (MB) medium containing 25% glycerol at −80°C. Six type strains, namely, *Mangrovivirga cuniculi* KCTC 72349^T, *Pontibacter actiniarum* KCTC 12367^T, *Pontibacter litorisediminis* KCTC 52252^T, *Poritiphilus flavus* MCCC 1K03853^T, *Eudoraea chungangensis* KCTC 42048^T, and *Zeaxanthinibacter enoshimensis* NBRC 101990^T, were purchased from the Korean Collection for Type Cultures (KCTC), the Marine Culture Collection of China (MCCC), and the NITE Biological Resource Center (NBRC), and used as reference strains in this study.

2.2 Morphological, physiological, and chemotaxonomic characteristics

Strains M17^T, M82^T, and M415^T were cultured on Marine Agar (MA) medium for 3 days to observe their morphological characteristics, including colonial size, shape, edge, bulge, transparency, and color characteristics. Cell morphology, size, and special structure were examined using a transmission electron microscope (JEM-1230; JEOL). Gram staining reaction was performed according to the method described by Dong and Cai (Dong and Cai, 2001). Motility of the strains was assessed in semisolid MB medium containing 0.5% agar. The growth range and optimum temperature of the strains were determined in MB medium at 4°C, 10°C, 20°C, 25°C, 28°C, 30°C, 37°C, 40°C, 45°C, and 50°C, whereas their growth and optimal pH range were measured by adding appropriate buffer (40 mM) to MB medium (0.5 pH unit intervals), which include MES (pH 5.0–5.5), MOPS (pH 6.0–7.5), Tricine buffers (pH 8.0–8.5), and CAPSO (pH 9.0–10.0). By adding 0%, 0.5%, 1%, 1.5%, 2%, 2.5%, 3%, 3.5%, 4%, 6%, 8%, 10%, and 12% (w/v) NaCl to saltness-MB medium, the growth and optimal salinity range were determined. The optimal growth conditions and growth range were determined after 3 days and 1 month of culture, respectively. The growth condition of the strains was measured using a UV/visible spectrophotometer (Ultrospec 6300 Pro, Amersham Biosciences) at OD_{600}.

Sodium nitrate (20 mM) was used as a potential electron acceptor to assess the anaerobic growth of strains in the anaerobic system (AnaeroPack-MicroAero, 2.5 L, MGC, Japan) (Shi et al., 2017). Catalase activity was measured by dripping 3%

(v/v) hydrogen peroxide solution to the colonies placed on sterile slides. Oxidase activity was determined by observing whether the cell color turned red within 1 min after dripping 1% *p*-amino dimethylaniline oxalate solution. Carotenoid was extracted by acetone/methanol (7:2, v/v) solution, and their absorption spectra were determined using a scanning UV/visible spectrophotometer (Bowman and Nichols, 2005). Strains were cultured in suitable medium containing sodium thiosulfate (5 g/L), and their hydrogen sulfide production capacity was determined using sterile filter strips soaked in the solution of lead acetate. Amylase, cellulase, and hydrolysis of Tweens 20, 40, 60, and 80 were carried out according to the previously described methods (Liu et al., 2019). Carbon source oxidation was tested using Biolog GEN III MicroPlates, and activity of other common bacterial enzymes was examined using the API ZYM kit. Other physiological characteristics of the strains were analyzed using the API 20NE kit. All of the BIOLOG and API tests were carried out according to the manufacturer's instructions except for adjusting salinity to 2%.

Strains M17^T, M82^T, and M415^T and the six type strains were cultured on MB medium under optimal conditions, and the cells at the end of exponential growth stage were collected for chemotaxonomic analysis. Bacteria were collected and freeze-dried, then saponified, methylated, extracted, and washed to obtain the bacterial fatty acids (Sasser, 1990). Identification and quantification of the extracted cellular fatty acids of these strains were performed using a gas chromatograph (Agilent G6890N) and the Sherlock Microbial Identification System (MIDI database: Version 6.0). Polar lipids were extracted according to the procedure described by Minnikin et al. (1984), and composition analysis was performed on silica gel 60 F254 plates (10 × 10 cm, Merck) (Komagata and Suzuki, 1988). Isoprenoid quinones were extracted by a mixture of chloroform:methanol (2:1 v/v), and the further identification was performed by the HPLC-MS system.

2.3 16S rRNA gene sequence similarities and phylogenetic analysis

A total of 352 strains were isolated from 34 sampling stations. The 16S rRNA gene was amplified by PCR using the universal primers 27F/1492R and sequenced by Guangdong Magigene Biotechnology Co., Ltd. (Guangzhou, China). The sequences were submitted to NCBI under the accession numbers OQ617539–OQ617890. The complete 16S rRNA gene sequences of strains M17^T, M82^T, and M415^T were extracted from their draft genomes. The similarities of all 16S rRNA gene sequences were identified by aligning these sequences against the National Center for Biotechnology Information (NCBI) database (https://www.ncbi.nlm.nih.gov/) and the EzBioCloud database (https://www.ezbiocloud.net/).

The 16S rRNA gene sequence alignment of strains M17^T, M82^T, and M415^T and their phylogenetically related taxa were performed by the ClustalW algorithm within MEGA11 v11.0.13 (Tamura et al., 2021), and the phylogenetic trees were reconstructed by the neighbor-joining (NJ), maximum-parsimony (MP), and maximum-likelihood (ML) algorithms within the MEGA11 software (Felsenstein, 1981; Saitou and Nei, 1987). The robustness of phylogenetic trees was assessed through bootstrap analysis based on 1,000 replications.

2.4 Genome sequencing and analysis

The genomes of strains M17^T, M82^T, and M415^T were extracted using a bacterial genomic DNA kit (Takara), and draft genomes were sequenced using the Illumina NovaSeq 6000 platform (PE150) in Guangdong Magigene Biotechnology Co., Ltd. (Guangzhou, China). The sequences were assembled using SPAdes v3.10.1 (Zou et al., 2020), and the completeness and contamination of the assembled draft genomes were accessed using CheckM v1.1.3 (Parks et al., 2015).

Phylogenomic analysis based on single-copy orthologous clusters (OCs) of strains M17^T, M82^T, and M415^T and the related type strains were performed as described (Xu et al., 2018). Briefly, the orthologous clusters were filtered based on the blastp+ program and 50% sequence identity using Proteinortho v5.16 (Lechner et al., 2011), and their formats were converted into OrthoMCL for subsequent analysis. The single-copy orthologous clusters were aligned through MAFFT v7.310 (Katoh and Standley, 2013), and the aligned sequences were concatenated after further refining by trimAL v1.4.1 (Capella-Gutierrez et al., 2009). The IQ-TREE v1.6.2 software was used to predict the best-fit models. The phylogenetic trees were constructed by maximum-likelihood algorithms based on the concatenated aligned single-copy orthologous clusters (Lam-Tung et al., 2015), and the best-fit models of strains M17^T, M82^T, and M415^T were LG+F+R6, LG+F+R5, and LG+F+R8, respectively. Finally, MEGA11 software was employed to visualize the phylogenetic trees.

Functional and metabolic pathway predictions were realized by Kyoto Encyclopedia of Genes and Genomes (KEGG) and Evolutionary Genealogy of Genes with enhanced Non-supervised Orthologous Groups (EggNOG) (Kanehisa et al., 2017; Hernández-Plaza et al., 2023). The Average Nucleotide Identity (ANI) was calculated using the online ANI calculator based on the OrthoANIu algorithm, which is an improved iteration of the original OrthoANI algorithm (Yoon et al., 2017). Digital DNA–DNA hybridization (dDDH) and Two-way Average Amino Acid Identity (AAI) were calculated through Genome-to-Genome Distance Calculator 3.0 and the AAI calculator, respectively (Rodriguez-R and Konstantinidis, 2014; Meier-Kolthoff et al., 2022).

As for the potential in polysaccharide metabolism of strains M17^T, M82^T, and M415^T, carbohydrate-active enzymes (CAZymes) were predicted by the HMMER tools within dbCAN2 software based on Carbohydrate-Active enZYmes Database V11 (CAZy database), and SusC/D-like proteins (SusC, outer membrane TonB-dependent transporter; SusD, surface glycan-binding protein) and other auxiliary proteins and genes were predicted and annotated using PROKKA v1.12 and Rapid Annotation using Subsystem Technology (RAST) version 2.0 (Aziz et al., 2008; Seemann, 2014; Zhang et al., 2018; Drula et al., 2022). The PUL prediction relies on the identification in each genome of the PUL markers: the presence of adjacent genes encoding SusC/D-like proteins, and according to the position of CAZymes and SusC/D-

like proteins in the genome, combined with the position of corresponding auxiliary proteins and genes (Terrapon et al., 2015). In addition, the substrates of these PULs were predicted by searching through the PUL database (PULDB) and BLAST the CAZymes through UniProt (Terrapon et al., 2018; Consortium, 2019).

3 Results and discussion

3.1 Diversity of culturable bacteria in bare tidal flats

The sampling stations are widely distributed in the bare tidal flats of China. The samples from 34 sampling stations were used for the isolation of strains (Figure 1). A total of 352 bacterial strains were isolated. Compared with the 16S rRNA gene sequences with validly published species, the isolates were assigned to 180 species, belonging to 4 phyla, 7 classes, 22 orders, 37 families, and 94 genera; among them, 126 species and 52 genera had only one isolate (Table 1 and Figure 2). In our study, a higher number of species were discovered among the culturable strains compared with mangrove sediments (116 pure culture strains distributed in 13 species, 1 sample; Sefrji et al., 2022), plant rhizosphere (59 pure culture strains distributed in 22 species, 4 samples; Brígido et al., 2019), and Tabernas Desert (236 strains distributed in 37 genera, 3 samples; Molina-Menor et al., 2021); our results showed that bare tidal flats had a greater diversity of culturable bacteria. *Flavobacteriales* and *Bacillales* represented two most abundant orders, accounting for approx. 50% of the total isolates (Figure 3). A total of 17 strains were identified as *Fictibacillus phosphorivorans*, which was widely distributed in 12 sampling stations located in the different areas such as Jiangsu Province, Zhejiang Province, Guangxi Zhuang Autonomous Region, and Shanghai City. It became the most abundant and widely distributed culturable species in this study. Recent studies showed that *Fictibacillus phosphorivorans* was able to produce biosurfactant and displayed high nematicidal capability against root-knot nematodes (RKNs), which could infect almost all crops and lead to huge economic losses in agriculture around the world (Zheng et al., 2016; Pandey et al., 2021).

In addition, the effects of different depths and substrates on culturable bacteria were compared (Table 1). *Actinomycetota* strains, a total of 13 species in 5 orders, were isolated only in 0–5-cm non-sandy sediment, some of which were reported to have great ecological functions and economic values; e.g., strains of *Rhodococcus qingshengii* and *Brachybacterium paraconglomeratum* have the ability to repair heavy metal pollution (Du et al., 2022; Harboul et al., 2022) and pesticide contamination (Chuang et al., 2021; Wang et al., 2021), strains of *Arthrobacter pascens*, known as indole-3-acetic acid (IAA)-producing bacteria, could regulate plant growth and development (Li et al., 2021), and strains of *Cellulosimicrobium cellulans* are able to produce ginsenoside Rg3, a known anticancer agent (Hu et al., 2019). Different from *Actinomycetota* species, *Pseudomonadota* species *Psychrobacter nivimaris* was the only species distributed in all three types of sediment (Supplementary Figure 1), and strains in it may have the ecological function of repairing heavy metal pollution (Staloch et al., 2022).

In addition, a large number of novel species were discovered in bare tidal flats; a total of 47 strains showed less than 98.65% sequence similarities of the 16S rRNA gene with validly published species and may represent novel species (Kim et al., 2014). Most of them were assigned to *Cytophagales* and *Flavobacteriales*, both of which belong to the phylum *Bacteroidota*, with ratios of 46.2% and 30.2%, respectively. Three *Bacteroidota* strains (M17^T, M82^T, and M415^T) were chosen for further phylogenetic and functional characterization.

3.2 Morphological, physiological, and chemotaxonomic characteristics

The morphological observations by transmission electron microscopy showed that the cells of strains M17^T, M82^T, and M415^T were slender and long (2.0–10.0 μm × 0.3–0.5 μm), ellipsoidal to ovoid (0.9–3.2 μm × 0.6–1.1 μm), and slender and long (1.8–8.0 μm × 0.3–0.5 μm), respectively (Supplementary Figure 2 - Figure 4). For strain M17^T, after 3 days of cultivation, the colony was round, 1–3 mm in diameter, and orange in color; mobility was not observed in the semisolid MB medium; and anaerobic growth and carotenoid production were not detected. The colony of M82^T was round, 1–2 mm in diameter, and red in color after 3 days of incubation; mobility was not observed in the semisolid MB medium; and anaerobic growth and carotenoid production were both observed. The colony of M415^T was round, 0.5 mm in diameter, and orange in color; mobility was not observed; and anaerobic growth and carotenoid production were detected. All

TABLE 1 Taxonomic profile of isolates in different depths and substrates.

Depth	Phylum	Class	Order	Family	Genus	Species	Strains
0–5 cm	4	7	22	37	88	165	295
5–15 cm	3	5	6	7	8	10	10
15–25cm	3	4	9	9	17	21	47
Substrate							
Mud	4	7	20	32	74	136	254
Sand	3	4	10	14	30	42	64
Muddy sand	4	5	11	13	21	26	34

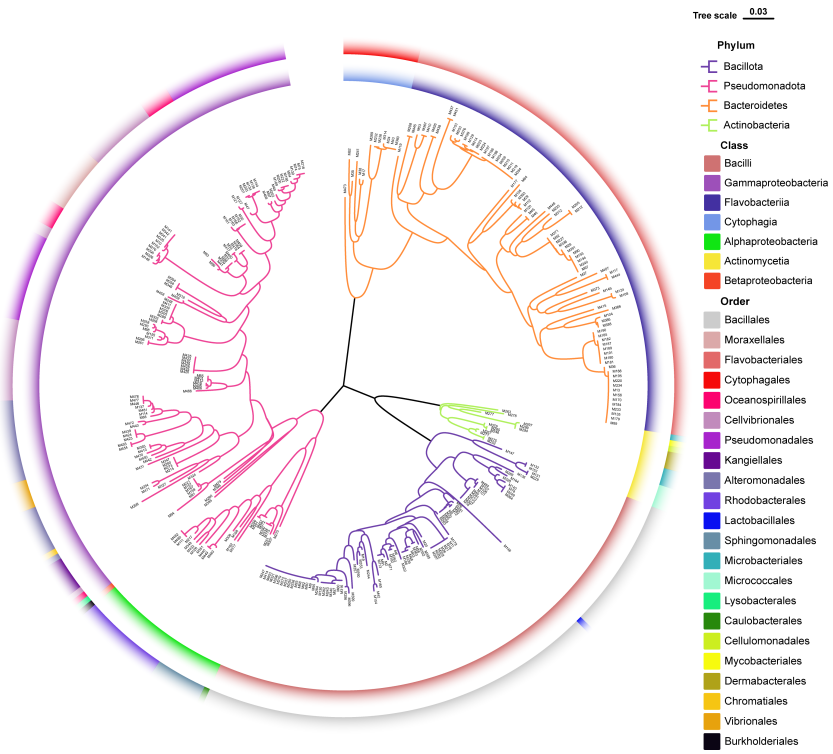

FIGURE 2
Diversity of culturable bacteria from unvegetated tidal flats of China. Neighbor-joining phylogenetic tree reconstructed from 16S rRNA gene sequences of 352 pure culture isolates. Branches in different colors represent different bacterial phyla; colors on the inner ring refer to bacterial classes; and colors on the outer ring refer to bacterial orders.

the three strains were positive in the oxidations of D-fucose, L-galactonic acid lactone, D-glucuronic acid, glucuronamide, and tetrazolium violet. Detailed differences between strains M17^T, M82^T, and M415^T and reference strains are summarized in Table 2 and Supplementary Table 1.

The major respiratory quinone of strains M17^T and M82^T was MK-7, which is consistent with their reference strains *Mangrovivirga cuniculi* KCTC 72349^T, *Pontibacter actiniarum* KCTC 12367^T, and *Pontibacter litoriseditiminis* KCTC 52252^T. The major respiratory quinone of strain M415^T was MK-6, identical with that of

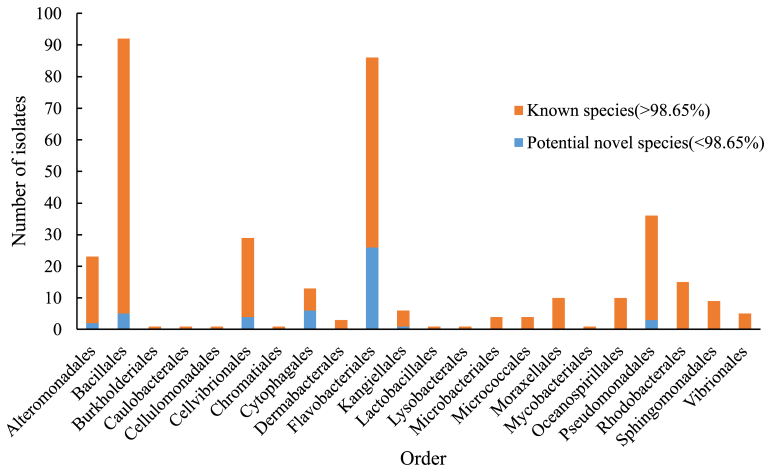

FIGURE 3
Number of isolates in different orders. Blue bar, the number of potential novel species in each order (16S rRNA gene similarity < 98.65%). Orange bar, the number of identified isolates in each order (16S rRNA gene similarity > 98.65%).

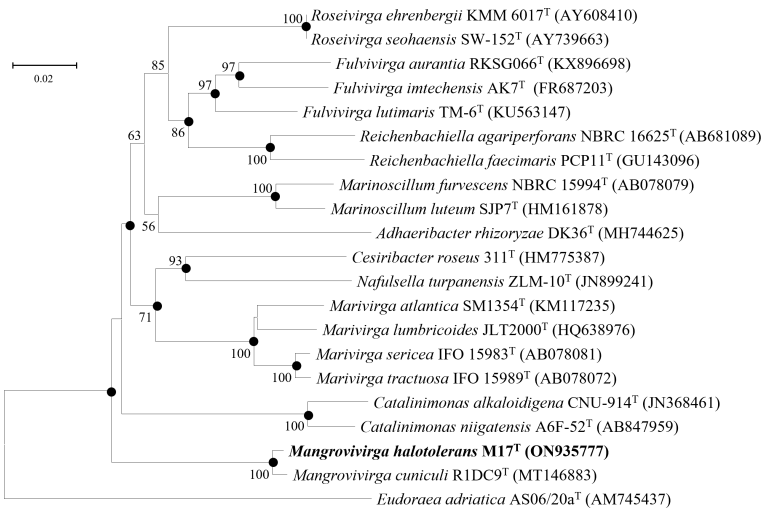

FIGURE 4
Neighbor-joining phylogenetic tree reconstructed from 16S rRNA gene sequences of strains M17^T and related species. Bootstrap values <50% (based on 1,000 replications) are not shown. Filled circles indicate branches that were also recovered using maximum-likelihood and maximum-parsimony methods. *Eudoraea adriatica* AS06/20a^T (AM745437) was used as the outgroup; bar, 0.02 nt substitutions per nucleotide position.

TABLE 2 Differential phenotypic characteristics between strains M17^T, M82^T, and M415^T and their reference strains.

Characteristics	1	2	3	4	5	6	7	8	9
Colony color*	O	R	O	O	O	O	Y	Y	Y
Temp. range (°C)	20-45	20-40	25-37	20-40[a]	6-43[b]	10-45[c]	16-40[d]	20-30[e]	15-33[f]
pH range	6.5-9	6-9	6-8	6-10[a]	NA	5.5-9[c]	5.5-11[d]	6.5-8.5[e]	6-10[f]
NaCl conc. (%)	0.5-10	0-8	1-4	3-11[a]	0-10[b]	0-8[c]	0-8[d]	2-6[e]	2-8[f]
Nitrate reduction	–	–	–	–	+	–	–	+	–
Oxidase	+	+	+	+	+	+	–	+	+
Enzyme activity:									
Chymotrypsin	+	+	+	+	w	+	+	–	+
α-Galactosidase	–	+	–	–	–	+	w	–	+
β-Galactosidase	–	w	–	–	–	+	+	–	+
β-Glucuronidase	+	–	–	+	–	–	+	–	–
α-Glucosidase	–	+	w	–	+	+	+	–	+
β-Glucosidase	+	+	+	w	–	+	+	–	+
N-Acetyl-glucosaminidase	+	+	+	–	+	+	+	+	+
α-Mannosidase	–	–	–	–	–	+	+	–	w
Hydrolysis of:									
Tween 20	–	–	–	–	+	–	–	–	–
Tween 40	–	–	–	–	–	–	w	–	+
Tween 60	–	–	–	–	–	–	+	–	+
Tween 80	–	–	–	+	+	–	+	–	–
Starch	+	–	w	+	–	–	w	+	+

(Continued)

TABLE 2 Continued

Characteristics	1	2	3	4	5	6	7	8	9
Oxidation of:									
D-Maltose	–	+	+	–	+	+	–	–	+
D-Cellobiose	–	+	+	–	+	+	–	–	+
Sucrose	w	+	+	–	–	w	–	–	+
α-D-Lactose	w	+	–	+	–	+	–	–	+
D-Salicin	–	+	+	–	–	+	–	–	+
N-Acetyl-D-glucosamine	–	+	+	–	+	+	–	–	+
L-Fucose	–	+	w	+	–	+	+	+	+
Fusidic acid	+	+	+	–	–	–	+	+	+
D-Glucose-6-PO_4	–	+	+	–	+	–	–	–	w
D-Galacturonic acid	w	+	w	+	+	+	+	+	+
Tetrazolium blue	–	+	–	+	–	–	+	+	–
Bromo-succinic acid	w	–	+	–	+	–	+	+	+
Acetoacetic acid	+	+	–	–	+	+	+	+	+
Acetic acid	+	+	–	–	+	+	–	–	–
Formic acid	+	+	–	–	–	–	–	w	–
Sodium butyrate	+	+	+	–	–	+	+	+	+

Strains: 1, M17^T; 2, M82^T; 3, M415^T; 4, Mangrovivirga cuniculi KCTC 72349^T; 5, Pontibacter actiniarum KCTC 12367^T; 6, Pontibacter litorisediminis KCTC 52252^T; 7, Zeaxanthinibacter enoshimensis NBRC 101990^T; 8, Eudoraea chungangensis KCTC 42048^T; 9, Poritiphilus flavus MCCC 1K03853^T. All data were obtained from this study unless stated otherwise. +, positive reaction; w, weakly positive reaction; -, negative reaction; NA, data not available. *Colony color in orange, red, and yellow are abbreviated as O, R, and Y, respectively. All strains are positive for the following characteristics: catalase, alkaline phosphatase, esterase (C4), esterase lipase (C8), leucine arylamidase, valine arylamidase, cystine arylamidase, trypsin, acid phosphatase, and naphthol-AS-BI-phosphohydrolase. All strains are negative for the following characteristics: Gram-staining, H_2S production, lipase (C14).
Data taken from the following: a, Sefrji et al. (Sefrji et al., 2021); b, Nedashkovskaya et al. (Nedashkovskaya et al., 2005); c, Park et al. (Park et al., 2016); d, Asker et al. (Asker et al., 2007); e, Siamphan et al. (Siamphan et al., 2015); f, Wang et al. (Wang et al., 2020a).

Poritiphilus flavus MCCC 1K03853^T, *Eudoraea chungangensis* KCTC 42048^T, and *Zeaxanthinibacter enoshimensis* NBRC 101990^T.

The main polar lipids of strain M17^T were phosphatidylethanolamine (PE), aminoglycolipid (AGL), one unidentified phospholipid (PL), three unidentified aminolipids (ALs), three unidentified glycolipids (GLs), and six unidentified lipids (L1–6) (Supplementary Figure 5). Compared with its reference strain *M. cuniculi* KCTC 72349^T, they both contained PE as main polar lipids, but strain M17^T comprised more polar lipids such as AGL, ALs, and GLs. The major polar lipids of strain M82^T were PE, two ALs, and nine unidentified lipids (L1–9), in which PE and plenty of unidentified lipids were also detected in other species of the genus *Pontibacter* (Nedashkovskaya et al., 2005; Zhang et al., 2008; Subhash et al., 2013; Park et al., 2016). The major polar lipids detected in M415^T were PE, phosphoglycolipid (PGL), aminophospholipid (APL), one GL, two ALs, and five unidentified lipids (L1–5).

Similar to *M. cuniculi* KCTC 72349^T, iso-$C_{15:0}$ and iso-$C_{17:0}$ 3-OH were the main cellular fatty acids (>10%) in strain M17^T. Meanwhile, strain M82^T contained iso-$C_{15:0}$ and summed feature 4 (SF4) as the major cellular fatty acids (>10%), which was also found in its reference strains. However, some differences in the ratio of main fatty acids (such as iso-$C_{15:0}$) existed between the two novel isolates and their reference strains (Table 3). Similar to its reference strains, strain M415^T contained iso-$C_{15:0}$ and iso-$C_{17:0}$ 3-OH as the main cellular fatty acids, but the relatively higher ratio of iso-$C_{15:1}$ -G and the lower ratio of summed feature 3 (SF3) differed strain M415^T from its reference strains (Table 3).

3.3 Phylogenetic analysis and genomic properties

The 16S rRNA gene sequences between strain M17^T and *M. cuniculi* KCTC 72349^T shared the highest similarity of 99.28%, and less than 90.09% with other species (Table 4). In both of the phylogenetic trees based on the 16S rRNA gene and single-copy orthologous clusters (concatenated protein sequences), strain M17^T formed a closest and robust cluster with *M. cuniculi* KCTC 72349^T (Figure 4 and Supplementary Figure 6), indicating that strain M17^T was affiliated with the genus *Mangrovivirga*. Although sequence similarity of the 16S rRNA gene reached 99.28% between strains M17^T and *M. cuniculi* KCTC 72349^T, the dDDH, ANI, and AAI values between strain M17^T and *M. cuniculi* KCTC 72349^T were 57.9%, 84.0%, and 88.8%, respectively (Table 4), all lower than the thresholds for species delimitation (Konstantinidis and Tiedje, 2005; Tindall et al., 2010; Kim et al., 2014), indicating that strain M17^T

10.3389/fmars.2023.1222157

TABLE 3 Cellular fatty acid composition of strains M17^T, M82^T, and M415^T and their reference strains.

Fatty acid	1	2	3	4	5	6	7	8	9
Saturated straight chain:									
$C_{12:0}$	TR	–	1.9	TR	–	–	–	–	–
$C_{14:0}$	TR	–	1.3	TR	–	–	TR	TR	TR
$C_{16:0}$	TR	TR	2.5	TR	TR	TR	3.1	3.6	4.5
$C_{18:0}$	–	TR	1.7	–	TR	TR	–	–	–
Saturated branched chain:									
iso-$C_{11:0}$	3.4	–	–	3.3	–	–	–	–	–
iso-$C_{13:0}$	1.2	TR	–	TR	TR	–	–	TR	TR
iso-$C_{15:0}$	43.3	25.8	22.7	35.7	32.2	22.3	24.9	18.7	25.1
anteiso-$C_{15:0}$	0.3	TR	TR	TR	TR	TR	3.8	3.2	0.4
iso-$C_{16:0}$	4.6	3.4	5.1	4.1	TR	TR	4.4	TR	1.0
iso-$C_{17:0}$	1.5	2.7	TR	1.5	5.5	2.6	TR	TR	TR
Unsaturated branched chain:									
iso-$C_{15:1}$ -G	9.9	–	24.4	10.9	–	–	7.0	13.0	14.1
iso-$C_{16:1}$ -G	1.0	–	1.2	TR	–	–	–	–	–
iso-$C_{16:1}$ -H	–	2.7	–	–	TR	TR	1.2	–	–
$C_{16:1\ \omega5c}$	6.2	–	–	4.7	–	3.2	–	–	–
$C_{17:1\ \omega6c}$	–	2.0	–	–	1.1	2.0	1.5	TR	–
$C_{17:1\ \omega8c}$	–	–	–	–	–	TR	1.3	TR	–
$C_{18:1\ \omega9c}$	0.4	1.2	–	TR	1.2	1.0	TR	TR	TR
Hydroxylated:									
iso-$C_{15:0}$ 3-OH	4.1	3.7	6.8	5.3	4.4	3.0	3.6	6.7	6.2
$C_{15:0}$ 2-OH	–	–	–	–	–	–	TR	1.2	TR
$C_{15:0}$ 3-OH	–	–	–	–	–	–	–	1.7	–
$C_{16:0}$ 3-OH	2.8	–	TR	3.7	–	–	TR	2.7	2.2
iso-$C_{16:0}$ 3-OH	1.2	TR	8.6	1.0	TR	TR	4.3	2.7	1.5
$C_{17:0}$ 2-OH	–	TR	–	–	–	TR	1.2	TR	TR
iso-$C_{17:0}$ 3-OH	10.7	10.7	16.4	15.0	10.2	7.9	15.3	14.9	29.9
Summed feature [a]:									
1	–	3.6	–	–	2.1	2.5	–	–	–
3	3.6	7.1	3.5	4.8	12.9	7.7	8.1	20.8	10.9
4	3.7	31.2	–	4.9	26.1	39.9	–	–	–
9	–	TR	–	–	1.1	1.8	13.5	3.3	–

Strains: 1, M17^T; 2, M82^T; 3, M415^T; 4, Mangrovivirga cuniculi KCTC 72349^T; 5, Pontibacter actiniarum KCTC 12367^T; 6, Pontibacter litorisediminis KCTC 52252^T; 7, Zeaxanthinibacter enoshimensis NBRC 101990^T; 8, Eudoraea chungangensis KCTC 42048^T; 9, Porithiphilus flavus MCCC 1K03853^T. All data were obtained from this study unless stated otherwise. Fatty acids representing trace amounts or not detected in all strains are not shown. TR, Trace amount (<1%); -, not detected; Fatty acids more than 10% of total were indicated in bold.

[a]Summed features represent groups of two or three fatty acids that could not be separated by GLC using the MIDI system. Summed feature 1 contains $C_{13:0}$ 3-OH and/or iso-$C_{15:1}$ H; summed feature 3 contains $C_{16:1}$ ω6c and/or $C_{16:1}$ ω7c; summed feature 4 contains ante-iso-$C_{17:1}$ B and/or iso-$C_{17:1}$ I; summed feature 9 contains iso-$C_{17:1}$ ω9c.

represents a new species within the genus *Mangrovivirga*. In addition, the cell morphology of the strain *M. cuniculi* KCTC 72349^T was short rod-shaped (1.0–1.2 μm × 0.3–0.5 μm; Sefrji et al., 2021), which was different from that of strain M17^T, showing a long rod shape (2.0–10.0 μm × 0.3–0.5 μm; Supplementary Figure 2). In addition, there were also a great number of differences between them in phenotypic and genomic properties (Tables 2-5). Therefore, strain M17^T represents a novel species of the genus *Mangrovivirga*.

TABLE 4 16S rRNA gene sequence similarities, digital DNA-DNA hybridization (dDDH), Average Nucleotide Identity (ANI), and Average Amino acid Identity (AAI) of strains M17^T, M82^T, and M415^T and their related type strains.

Reference genome	16S rRNA (%)	dDDH (%)	ANI (%)	AAI (%)
M17^T				
Mangrovivirga cuniculi KCTC 72349^T	99.28	57.9	83.97	88.82
Roseivirga spongicola JCM 13337^T	90.09	12.6	66.96	50.29
Marivirga sericea ATCC 23182^T	90.08	12.6	67.28	50.95
M82^T				
Pontibacter litorisediminis KCTC 52252^T	97.85	35.6	81.08	84.22
Pontibacter korlensis X14-1^T	97.43	23.2	77.89	82.1
Pontibacter actiniarum KCTC 12367^T	96.59	24.1	78.85	80.17
M415^T				
Eudoraea chungangensis KCTC 42048^T	93.68	13.2	68.84	66.94
Robiginitalea biformata KCTC 12146^T	93.08	12.9	69.08	65.37
Zeaxanthinibacter enoshimensis NBRC 101990^T	92.91	13	69.69	67.31
Eudoraea adriatica DSM 19308^T	92.62	13.5	69.43	69.35
Poritiphilus flavus MCCC 1K03853^T	92.44	13.1	70.23	68.33

Strain M82^T shares the highest 16S rRNA gene sequence similarity of 97.85%, 97.43%, and 96.59%, respectively, with *Pontibacter litorisediminis* KCTC 52252^T, *Pontibacter korlensis* X14-1^T, and *Pontibacter actiniarum* KCTC 12367^T, lower than the threshold for species delimitation (Kim et al., 2014). Based on the phylogenetic analysis of 16S rRNA gene sequences and single-copy orthologous clusters, strain M82^T was closely clustered within *Pontibacter* strains (Figure 5 and Supplementary Figure 7). The highest values of dDDH, ANI, and AAI between strain M82^T and the type strains within the genus *Pontibacter* were 35.6%, 81.1%, and 84.2%, respectively, which are lower than the thresholds of species delimitation (Table 4).

Low 16S rRNA gene sequence similarities were found between strain M415^T and its type species of the genera *Eudoraea* (92.62%–93.68%), *Zeaxanthinibacter* (92.02%–92.91%), *Muriicola* (92.21%–92.83%), *Robiginitalea* (91.48%–92.74%), and *Poritiphilus* (92.44%). Phylogenetic analysis based on 16S rRNA gene sequences and single-copy orthologous clusters showed that strain M415^T was clearly separated from the related genera (Figure 6 and Supplementary Figure 8), representing a novel species of a new genus within the family *Flavobacteriaceae*. The highest values of dDDH, ANI, and AAI between strain M415^T and its related species were 13.5%, 70.2%, and 69.4%, respectively (Table 4).

The genomic features of strains M17^T, M82^T, and M415^T and their related strains were analyzed to further confirm the taxonomic status of these three novel strains (Table 5). Strain M17^T showed a similar genome size and GC content with *M. cuniculi* KCTC 72349^T, but the latter has more protein-coding genes and obvious multicopy of the rRNA gene than strain M17^T. The genomic composition of strain M82^T was different from the related species, showing a higher GC content and a lower number of rRNA. Strain M415^T has the smallest genome size and the lowest protein-coding gene number, compared with its related species. According to the annotation result against the COG database, the most abundant category in strains M17^T and M82^T was cell wall/membrane/envelope biogenesis; however, in strain M415^T, it changed to amino acid transport and metabolism (Supplementary Figure 9). The genome sequences of strains M17^T, M82^T, and M415^T were annotated against the KEGG database and 1,614 (39.43%), 1,775 (44.55%), and 1,368 (47.14%) genes were assigned to putative functions, respectively. These functions were mainly composed of carbohydrate metabolism, genetic information processing, signaling and cellular processing, and amino acid metabolism, and notably, strain M82^T contained much more function genes associated with energy metabolism and environmental information processing (Supplementary Figure 10).

As indicated by KEGG pathway annotation, these three strains have many differences in metabolic pathways. As for sulfur metabolism, the assimilatory sulfate reduction (M00176) was devoid only in strain M415^T. In the lipid metabolism, phosphatidylcholine (PC) biosynthesis (M00091) was only found in strain M82^T; nevertheless, strain M82^T and strain M415^T both contained the threonine biosynthesis (M00018) which was not found in strain M17^T. In the metabolism of major nutrients, the complete β-oxidation pathway only existed in strain M17^T; the phosphate acetyltransferase-acetate kinase pathway was complete in strains M17^T and M415^T but incomplete in strain M82^T (Figure 7). In addition, we also found that the glyoxylate cycle was presented in both strains M17^T and M82^T but not in strain M415^T (Figure 7); the activation of the glyoxylate cycle could provide malic acid and

10.3389/fmars.2023.1222157

TABLE 5 Genomic statistics of strains M17^T, M82^T, and M415^T and their related type strains.

	1	2	3	4	5	6	7	8	9	10	11	12	13	14
Genome size (MB)	4.67	4.64	3.13	4.66	4.48	4.74	5.00	5.46	4.97	3.73	3.53	3.34	3.91	4.99
Completeness (%)	99.7	100	99.33	98.74	99.05	100	100	99.7	99.97	98.68	99.01	99.34	99.28	99.67
G+C content (%)	35.9	50.6	44.6	36.1	40.2	36.0	53.2	47.3	53.2	37.2	55.3	46.4	38.3	44.5
Genes (no.)	4,093	3,984	2,902	4,303	4,021	4,127	4,350	4,768	4,411	3,322	3,158	2,970	3,528	4,282
tRNA genes (no.)	38	43	39	43	40	41	43	49	51	36	41	38	37	40
rRNA genes (no.)	3	3	3	12	3	7	5	12	15	3	6	3	5	3
GenBank ID	JAPFQN00	JAPFQO00	JAPFQP00	CP028923	LRPC01	FXAW01	JARDUA00	CP009621	AXBP01	JARDUB00	CP001712	SNYI00	ARNE01	WXYO00

Strains: 1, M17^T; 2, M82^T; 3, M415^T; 4, Mangrovivirga cuniculi KCTC 72349^T; 5, Roseivirga spongicola JCM 13337^T; 6, Marivirga sericea ATCC 23182^T; 7, Pontibacter litoriseditinis KCTC 52252^T; 8, Pontibacter korlensis X14-1^T; 9, Pontibacter actiniarum KCTC 12367^T; 10, Eudoraea chungangensis KCTC 42048^T; 11, Robiginitalea biformata KCTC 12146^T; 12, Zeaxanthinibacter enoshimensis NBRC 101990^T; 13, Eudoraea adriatica DSM 19308^T; 14, Porifiphilus flavus MCCC 1K03853^T.

NADH, which serve as precursors and energy sources for metabolic reactions to sustain cell survival under stress conditions (Schroeter et al., 2011; Yuan et al., 2019). Therefore, the existence of the glyoxylate cycle for resisting the stress condition in tidal flats might indicate the adaptation mechanism of strains M17^T and M82^T to such environment.

3.4 The potential in polysaccharide metabolism

Considering the outstanding polysaccharide metabolic abilities of marine *Bacteroidota* (Krüger et al., 2019), especially *Flavobacteriaceae* strains (Kappelmann et al., 2019; Gavriilidou et al., 2020), and special geographical location of mudflats—the source of strains M17^T, M82^T, and M415^T, we further analyzed their CAZyme profiles and potential polysaccharide substrates. The result showed that strains M17^T, M82^T, and M415^T had 114, 155, and 103 CAZymes, respectively (Figure 8A), which were similar as the KEGG results, where 157, 175, and 153 genes for the carbohydrate metabolism pathway were detected, respectively. The detailed numbers of each CAZyme family presented in three strains are summarized in Supplementary Table 2. GH and GT were the most abundant CAZyme classes, accounting for more than 70% of the total CAZymes; this finding was consistent with studies on carbohydrate-active enzymes in *Flavobacteriaceae* species by Gavriilidou et al., which also indicated that GH and GT were the most abundant CAZyme classes (Gavriilidou et al., 2020). Strain M82^T comprised the highest number of CAZymes assigned to different classes and SusC/D-like proteins, indicating that it may have great potential in polysaccharide metabolism. However, the CAZyme count per Mb genome in strain M415^T was similar with strain M82^T and much higher than that in strain M17^T, even though the total number of CAZymes of strain M415^T was smaller than strains M17^T and M82^T due to the smallest genome size of strain M415^T (Figure 8B). A great number of GT2 and GT4 were present in strain M415^T, and they were involved in critical glycan synthesis, such as cellulose, chitin, and mannan; in addition, a higher number of GH2, GH3, GH16, and GH30 revealed that strain M415^T can metabolize plant polysaccharides and oligosaccharides (Coutinho et al., 2003; Gómez-Silva et al., 2019).

Polysaccharide utilization loci (PULs) are specialized saccharolytic systems that exhibit functional homology to the paradigmatic starch utilization system; the number and type of PULs determine the potential of polysaccharide utilization (Xu et al., 2003; McKee et al., 2021). According to the annotation results of carbohydrate-active enzymes and the SusC/D-like protein complex, we manually sorted the PULs of three novel strains (Figure 9); strains M17^T, M82^T, and M415^T have five, six, and two putative PULs, respectively. The PULs in strains M17^T and M82^T were specific for marine polysaccharide metabolism; for strain M17^T, PUL2 may be associated with the degradation of ulvan as the existence of GH2 (β-xylosidase), PUL3 may be associated with the degradation of laminarin as the existence of GH3 and GH16_3 (Tang et al., 2017; Chen et al., 2018), and PUL4 may be associated with the degradation of chitin as the

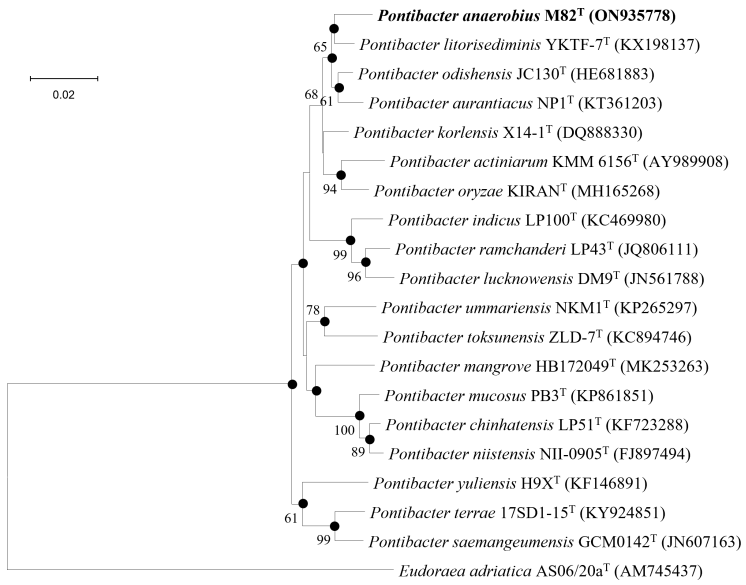

FIGURE 5
Neighbor-joining phylogenetic tree reconstructed from 16S rRNA gene sequences of strains M82^T and related species. Bootstrap values < 50% (based on 1,000 replications) are not shown. Filled circles indicate branches that were also recovered using maximum-likelihood and maximum-parsimony methods. *Eudoraea adriatica* AS06/20a^T (AM745437) was used as the outgroup; bar, 0.02 nt substitutions per nucleotide position.

existence of GH18 (Kappelmann et al., 2019). For strain M82^T, PUL1 may be associated with the degradation of fucoidan as the existence of GH29 (fucosidase) and PUL4 may be associated with the degradation of laminarin as the existence of GH16_3 (Tang et al., 2017; Chen et al., 2018). However, with the ability to utilize marine polysaccharides as strains M17^T and M82^T, strains M415^T can also utilize polysaccharides that are mainly present in land; for instance, it contained more glycogen and starch

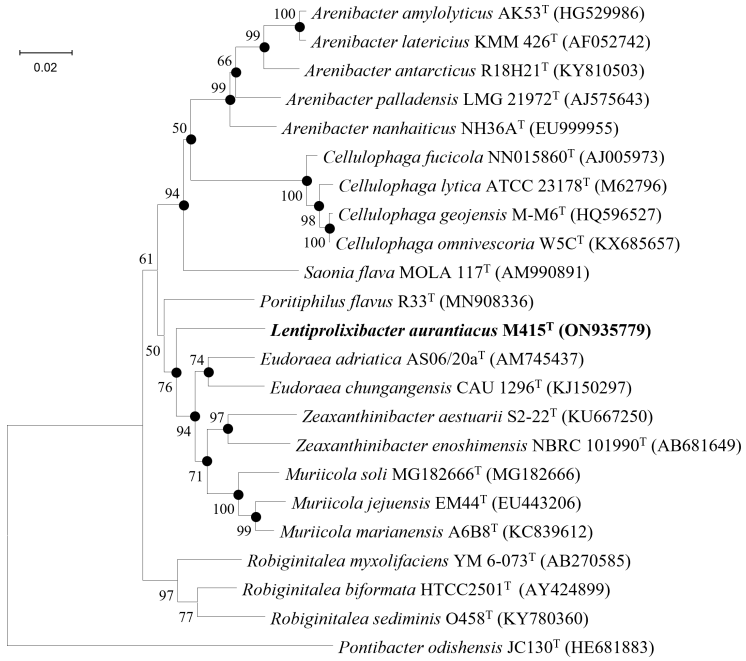

FIGURE 6
Neighbor-joining phylogenetic tree reconstructed from 16S rRNA gene sequences of strains M415^T and related species. Bootstrap values < 50% (based on 1,000 replications) are not shown. Filled circles indicate branches that were also recovered using maximum-likelihood and maximum-parsimony methods. *Pontibacter odishensis* JC130^T (HE681883) was used as the outgroup; bar, 0.02 nt substitutions per nucleotide position.

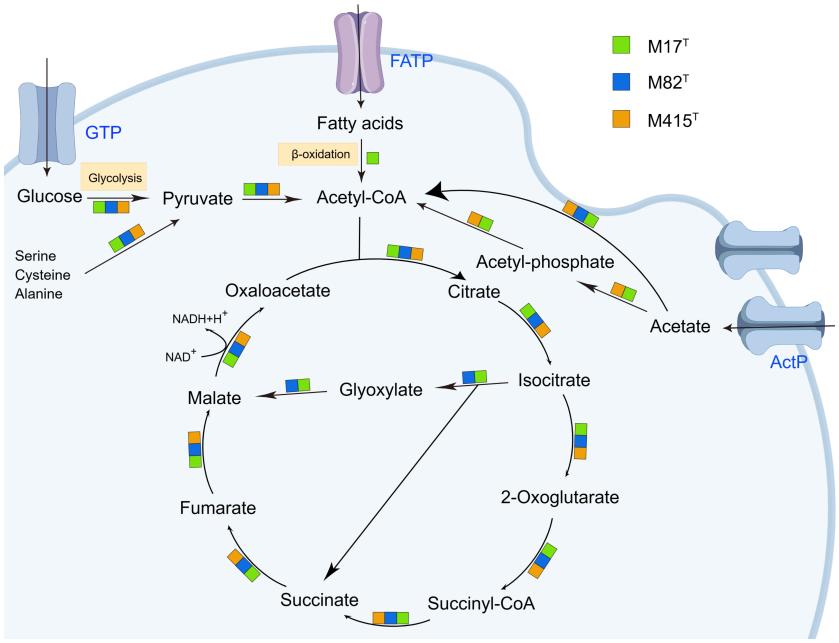

FIGURE 7
The citrate cycle (TCA cycle) and glyoxylate cycle in strains M17^T, M82^T, and M415^T. Color blocks indicated the reaction occurred in specific strains. GTP, glucose transport protein. FATP, fatty acid transport proteins. ActP, acetate permease. Other products have been omitted.

degrading CAZymes compared to another two strains (e.g., GH13, GH13_8; Berlemont and Martiny, 2015), and the PUL1 of strain M415^T may be related to the degradation of glycogen or starch.

3.5 Description of *Lentiprolixibacter* gen. nov.

Lentiprolixibacter (L. masc. adj. *lentus*, slow, delayed; L. masc. adj. *prolixus*, long, extended; N.L. masc. n. *bacter*, a rod; N.L. masc. n. *Lentiprolixibacter*, slowly growing long rod)

Cells are Gram-stain-negative, non-spore-forming, and non-motile aerobic rods. Catalase- and oxidase-positive. Predominant menaquinone is menaquinone 6 (MK-6). Major polar lipids are phosphatidylethanolamine, phosphoglycolipid, aminophospholipid, unidentified glycolipids, aminolipids, and lipids. The type species is *Lentiprolixibacter aurantiacus*.

3.6 Description of Lentiprolixibacter aurantiacus sp. nov.

Lentiprolixibacter aurantiacus (au.ran.ti.a'cus. N.L. masc. adj. *aurantiacus*, orange-colored)

Displays the following characteristics in addition to those given in the genus description. Cells are rod shaped and usually 0.3–0.5 μm wide and 1.8–8.0 μm long. Colonies (0.5 mm in diameter) are circular, convex, smooth, shiny, and orange pigmented after 3 days of incubation. Cells grow at 25°C–37°C (optimum, 25°C–30°C) in a

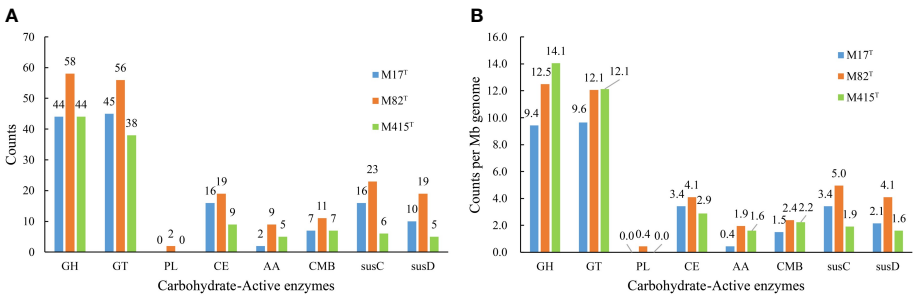

FIGURE 8
The number of predicted carbohydrate-active enzymes in strains M17^T, M82^T, and M415^T. **(A)** number of predicted CAZymes per genome and **(B)** average number of predicted CAZymes per Mb genome. GH, glycoside hydrolases; GT, glycosyltransferases; PL, polysaccharide lyases; CE, carbohydrate esterases; AA, auxiliary activities; CBM, carbohydrate-binding modules.

10.3389/fmars.2023.1222157

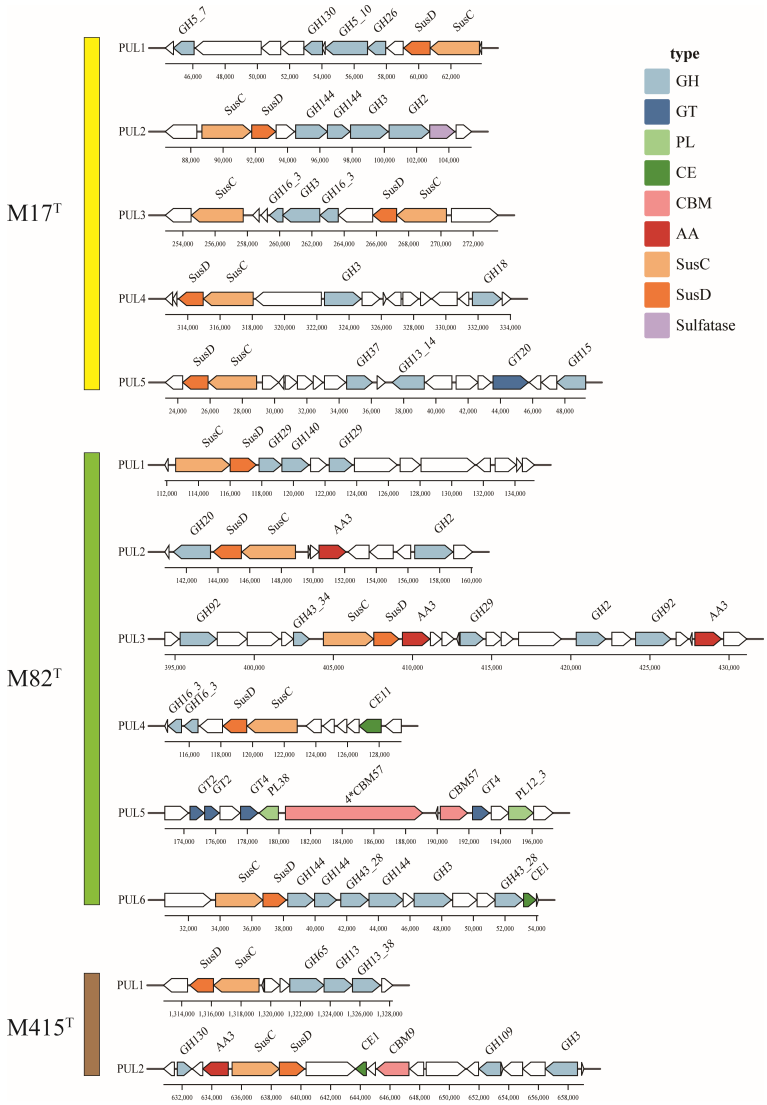

FIGURE 9
The putative polysaccharide utilization loci and genes in strains M17^T, M82^T, and M415^T. GH, glycoside hydrolases; GT, glycosyltransferases; PL, polysaccharide lyases; CE, carbohydrate esterases; AA, auxiliary activities; CBM, carbohydrate-binding modules.

medium of pH 6–8 (optimum, pH 6.5–7) and contain 1%–4% NaCl (optimum, 2%–3%). Catalase and oxidase are positive; nitrate reduction, carotenoid production, and H_2S production are negative. Starch is weakly hydrolyzed, but Tweens 20, 40, 60, and 80 are not. Dextrin, D-maltose, D-trehalose, D-cellobiose, gentiobiose, sucrose, D-turanose, β-methyl-D-glucoside, D-salicin, *N*-acetyl-D-glucosamine, α-D-glucose, fusidic acid, D-serine, D-glucose-6-PO_4, D-fructose-6-PO_4, pectin, glucuronamide, L-malic acid, bromo-succinic acid, nalidixic acid, and sodium butyrate are oxidized. In assays with the API ZYM system, alkaline phosphatase, esterase (C4), esterase lipase (C8), leucine arylamidase, valine arylamidase, cystine arylamidase, trypsin, chymotrypsin, acid phosphatase, naphthol-AS-BI-phosphohydrolase, β-glucosidase, and *N*-acetylglucosaminidase are positive and α-glucosidase is weakly positive. The major cellular fatty acids (>10%) are iso-$C_{15:0}$, iso-$C_{15:1}$ -G, and iso-$C_{17:0}$ 3-OH. The polar lipids are phosphatidylethanolamine, phosphoglycolipid, aminophospholipid, one unidentified glycolipids, two unidentified aminolipids, and five unidentified lipids. The DNA G+C content of the type strain is 44.6%.

The type strain, M415^T (MCCC 1K08058^T = KCTC 92534^T), was isolated from an intertidal mudflat (0–5 cm) collected from Taizhou, Zhejiang Provence, PR China. The GenBank accession numbers for the 16S rRNA gene sequence and the draft genome sequence of strain M415^T are ON935779 and JAPFQP000000000, respectively.

3.7 Description of *Mangrovivirga halotolerans* sp. nov.

Mangrovivirga halotolerans (ha.lo.to'le.rans. Gr. masc. n. *hals*, salt; L. pres. part. *tolerans*, tolerating, enduring; N.L. part. adj. *halotolerans*, salt-tolerating)

Cells are Gram-stain negative, non-motile, strictly aerobic rod-shaped, usually 0.3–0.5 μm wide, and 2–10 μm long, some more than 10 μm in length. Colonies (1–3 mm in diameter) are circular, convex, smooth, shiny, and orange pigmented after 3 days of incubation. Cells grow at 20°C–45°C (optimum, 20°C–28°C) in a medium of pH 6.5–9 (optimum, pH 6.5-7.5) and contain 0.5%–10% NaCl (optimum, 3.5%–6%). Catalase and oxidase activities are positive; nitrate reduction, carotenoid production, and H_2S production are negative. Starch is hydrolyzed, but Tweens 20, 40, 60, and 80 are not. Sucrose, stachyose, D-fucose, fusidic acid, L-alanine, glucuronamide, tetrazolium violet, α-keto-glutaric acid, L-malic acid, nalidixic acid, acetoacetic acid, propionic acid, acetic acid, formic acid, aztreonam, and sodium butyrate are oxidized. In assays with the API ZYM system, alkaline phosphatase, esterase (C4), esterase lipase (C8), leucine arylamidase, valine arylamidase, cystine arylamidase, trypsin, chymotrypsin, acid phosphatase, naphthol-AS-BI-phosphohydrolase, β-glucuronidase, β-glucosidase, and *N*-acetylglucosaminidase are positive. The predominant menaquinone is MK-7. The major cellular fatty acids (>10%) are iso-$C_{15:0}$ and iso-$C_{17:0}$ 3-OH. The polar lipids are phosphatidylethanolamine, aminoglycolipid, one unidentified phospholipid, three unidentified aminolipids, three unidentified glycolipids, and six unidentified lipids. The DNA G+C content of the type strain is 35.9%.

The type strain, M17^T (MCCC 1K08105^T = KCTC 92592^T), was isolated from an intertidal mudflat (0–5 cm) collected from Qingdao, Shandong Provence, PR China. The GenBank accession numbers for the 16S rRNA gene sequence and the draft genome sequence of strain M17^T are ON935777 and JAPFQN000000000, respectively.

3.8 Description of *Pontibacter anaerobius* sp. nov.

Pontibacter anaerobius (an.ae.ro'bi.us. Gr. pref. *an-*, not; Gr. masc. n. *aêr*, air; Gr. masc. n. *bios*, life; N.L. masc. adj. *anaerobius*, able to live in the absence of oxygen)

Cells are Gram-stain negative, non-motile, facultative aerobic rod-shaped, and usually 0.6–1.1 μm wide and 0.9–3.2 μm long. Colonies (1–2 mm in diameter) are circular, convex, smooth, shiny, and red pigmented after 3 days of incubation. Cells grow at 20°C–40°C (optimum, 28°C–37°C) in a medium of pH 6–9 (optimum, pH 6.5–7.5) and contain 0%–8% NaCl (optimum, 2%–3%). Carotenoid production and catalase and oxidase activity are positive. Nitrate reduction and H_2S production are negative. Starch and Tweens 20, 40, 60, and 80 are not hydrolyzed. Dextrin, D-maltose, D-trehalose, D-cellobiose, gentiobiose, sucrose, D-turanose, stachyose, D-raffinose, α-D-lactose, D-melibiose, β-methyl-D-glucoside, D-salicin, *N*-acetyl-D-glucosamine, α-D-glucose, D-mannose, D-galactose, D-fucose, L-fucose, fusidic acid, D-arabitol, myo-inositol, D-glucose-6-PO_4, D-fructose-6-PO_4, gelatin, glycyl-L-proline, L-aspartic acid, L-glutamic acid, L-serine, D-galacturonic acid, glucuronamide, acetoacetic acid, acetic acid, formic acid, and sodium butyrate are oxidized. In assays with the API ZYM system, alkaline phosphatase, esterase (C4), esterase lipase (C8), leucine arylamidase, valine arylamidase, cystine arylamidase, trypsin, chymotrypsin, acid phosphatase, α-galactosidase, α-glucosidase, β-glucosidase, and *N*-acetylglucosaminidase are positive; naphthol-AS-BI-phosphohydrolase and β-galactosidase are weakly positive. The predominant menaquinone is MK-7. The major cellular fatty acids (>10%) are iso-$C_{15:0}$, iso-$C_{17:0}$ 3-OH, and summed feature 4 (ante-iso-$C_{17:1}$ B and/or iso-$C_{17:1}$ I). The polar lipids are phosphatidylethanolamine, two unidentified aminolipids, and nine unidentified lipids. The DNA G+C content of the type strain is 50.6%.

The type strain, M82^T (MCCC 1K08048^T = KCTC 92537^T), was isolated from an intertidal mudflat (0–5 cm) collected from Taizhou, Zhejiang Provence, PR China. The GenBank accession numbers for the 16S rRNA gene sequence and the draft genome sequence of strain M82^T are ON935778 and JAPFQO000000000, respectively.

Data availability statement

The datasets presented in this study can be found in online repositories. The names of the repository/repositories and accession number(s) can be found in the article/Supplementary Material.

Author contributions

K-JM, Y-LY, and Y-HF collected the samples and isolated these strains. K-JM performed data collection and analysis. G-YF performed project guidance. K-JM and CS wrote the manuscript. X-WX and CS performed project guidance and critical revision of manuscripts. All authors contributed to the article and approved the submitted version.

Funding

This work was supported by the National Science and Technology Fundamental Resources Investigation Program of China (2019FY100700), the National Natural Science Foundation of China (No. 31900003), and the Key R&D Program of Zhejiang (#2023C03011).

Acknowledgments

We appreciate the helpful suggestion of Prof. Aharon Oren on the nomenclature and the help of Dr. Zhi-Cheng Wu and Dr. Maripat Xamxidin in sample collection and detection of polar lipids, respectively.

Conflict of interest

Author CS was employed by company Zhejiang Sci-Tech University Shaoxing Academy of Biomedicine Co., Ltd..

The remaining authors declare that the research was conducted in the absence of any commercial or financial relationships that could be construed as a potential conflict of interest.

Publisher's note

All claims expressed in this article are solely those of the authors and do not necessarily represent those of their affiliated organizations, or those of the publisher, the editors and the reviewers. Any product that may be evaluated in this article, or claim that may be made by its manufacturer, is not guaranteed or endorsed by the publisher.

Supplementary material

The Supplementary Material for this article can be found online at: https://www.frontiersin.org/articles/10.3389/fmars.2023.1222157/full#supplementary-material

References

Amann, R. I., Ludwig, W., and Schleifer, K. H. (1995). Phylogenetic identification and in *situ* detection of individual microbial cells without cultivation. *Microbiological Rev.* 59 (1), 143–169. doi: 10.1128/mmbr.59.1.143-169.1995

Asker, D., Beppu, T., and Ueda, K. (2007). *Zeaxanthinibacter enoshimensis* gen. nov., sp nov., a novel zeaxanthin-producing marine bacterium of the family *Flavobacteriaceae*, isolated from seawater off Enoshima Island, Japan. *Int. J. Systematic Evolutionary Microbiol.* 57 (4), 837–843. doi: 10.1099/ijs.0.64682-0

Aziz, R. K., Bartels, D., Best, A. A., DeJongh, M., Disz, T., Edwards, R. A., et al. (2008). The RAST server: Rapid annotations using subsystems technology. *BMC Genomics* 9 (1), 75. doi: 10.1186/1471-2164-9-75

Barbeyron, T., Thomas, F., Barbe, V., Teeling, H., Schenowitz, C., Dossat, C., et al. (2016). Habitat and taxon as driving forces of carbohydrate catabolism in marine heterotrophic bacteria: example of the model algae-associated bacterium Zobellia galactanivorans DsijT. *Environ. Microbiol.* 18 (12), 4610–4627. doi: 10.1111/1462-2920.13584

Bauer, J. E., Cai, W. J., Raymond, P. A., Bianchi, T. S., Hopkinson, C. S., and Regnier, P. A. (2013). The changing carbon cycle of the coastal ocean. *Nature* 504 (7478), 61–70. doi: 10.1038/nature12857

Berlemont, R., and Martiny, A. C. (2015). Genomic potential for polysaccharide deconstruction in bacteria. *Appl. Environ. Microbiol.* 81 (4), 1513–1519. doi: 10.1128/aem.03718-14

Bowman, J. P., and Nichols, D. S. (2005). Novel members of the family *Flavobacteriaceae* from Antarctic maritime habitats including *Subsaximicrobium wynnwilliamsii* gen. nov., sp. nov., *Subsaximicrobium saxinquilinus* sp. nov., *Subsaxibacter broadyi* gen. nov., sp. nov., *Lacinutrix copepodicola* gen. nov., sp. nov., and novel species of the genera *Bizionia*, *Gelidibacter* and *Gillisia*. *Int. J. Systematic Evolutionary Microbiol.* 55 (4), 1471–1486. doi: 10.1099/ijs.0.63527-0

Brígido, C., Singh, S., Menéndez, E., Tavares, M. J., Glick, B. R., Félix, M. D. R., et al. (2019). Diversity and functionality of culturable endophytic bacterial communities in chickpea plants. *Plants* 8 (2), 42. doi: 10.3390/plants8020042

Capella-Gutierrez, S., Silla-Martinez, J. M., and Gabaldon, T. (2009). trimAl: a tool for automated alignment trimming in large-scale phylogenetic analyses. *Bioinformatics* 25 (15), 1972–1973. doi: 10.1093/bioinformatics/btp348

Chang, M. X., Li, P., Li, Z. H., and Wang, H. J. (2022). Mapping tidal flats of the bohai and yellow seas using time series sentinel-2 images and google earth engine. *Remote Sens.* 14 (8), 1789. doi: 10.3390/rs14081789

Chen, J., Robb, C. S., Unfried, F., Kappelmann, L., Markert, S., Song, T., et al. (2018). Alpha- and beta-mannan utilization by marine Bacteroidetes. *Environ. Microbiol.* 20 (11), 4127–4140. doi: 10.1111/1462-2920.14414

Chernysheva, N., Bystritskaya, E., Stenkova, A., Golovkin, I., Nedashkovskaya, O., and Isaeva, M. (2019). Comparative Genomics and CAZyme Genome Repertoires of Marine Zobellia amurskyensis KMM 3526T and Zobellia laminariae KMM 3676T. *Mar. Drugs* 17 (12), 661. doi: 10.3390/md17120661

Choi, H. J., Jeong, T. Y., Yoon, H., Oh, B. Y., Han, Y. S., Hur, M. J., et al. (2018). Comparative microbial communities in tidal flats sediment on Incheon, South Korea. *J. Gen. Appl. Microbiol.* 64 (5), 232–239. doi: 10.2323/jgam.2017.12.007

Chuang, S. C., Yang, H. X., Wang, X., Xue, C., Jiang, J. D., and Hong, Q. (2021). Potential effects of *Rhodococcus qingshengii* strain djl-6 on the bioremediation of carbendazim-contaminated soil and the assembly of its microbiome. *J. Hazardous Materials* 414, 125496. doi: 10.1016/j.jhazmat.2021.125496

Consortium, U. (2019). UniProt: a worldwide hub of protein knowledge. *Nucleic Acids Res.* 47 (D1), D506–D515. doi: 10.1093/nar/gky1049

Coutinho, P. M., Deleury, E., Davies, G. J., and Henrissat, B. (2003). An evolving hierarchical family classification for glycosyltransferases. *J. Mol. Biol.* 328 (2), 307–317. doi: 10.1016/s0022-2836(03)00307-3

Dong, X. Z., and Cai, M. Y. (2001). "Determination of Biochemical Characteristics," in *Manual for the Systematic Identification of General Bacteria*. Eds. X. Z. Dong and M. Y. Cai (Beijing: Science Press), 370–398.

Drula, E., Garron, M. L., Dogan, S., Lombard, V., Henrissat, B., and Terrapon, N. (2022). The carbohydrate-active enzyme database: functions and literature. *Nucleic Acids Res.* 50 (D1), D571–D577. doi: 10.1093/nar/gkab1045

Du, S. T., Lu, Q., Liu, L. J., Wang, Y., and Li, J. X. (2022). *Rhodococcus qingshengii* facilitates the phytoextraction of Zn, Cd, Ni, and Pb from soils by Sedum alfredii Hance. *J. Hazardous Materials* 424, 127638. doi: 10.1016/j.jhazmat.2021.127638

Ettwig, K. F., Butler, M. K., Le Paslier, D., Pelletier, E., Mangenot, S., Kuypers, M. M., et al. (2010). Nitrite-driven anaerobic methane oxidation by oxygenic bacteria. *Nature* 464 (7288), 543–548. doi: 10.1038/nature08883

Felsenstein, J. (1981). Evolutionary trees from DNA sequences: A maximum likelihood approach. *J. Mol. Evol.* 17 (6), 368–376. doi: 10.1007/bf01734359

Fernández-Gómez, B., Richter, M., Schüler, M., Pinhassi, J., Acinas, S. G., González, J. M., et al. (2013). Ecology of marine Bacteroidetes: a comparative genomics approach. *ISME J.* 7 (5), 1026–1037. doi: 10.1038/ismej.2012.169

Folk, R. L., Andrews, P. B., and Lewis, D. W. (1970). Detrital sedimentary rock classification and nomenclature for use in New Zealand. N. Z. *J. Geology Geophysics* 13 (4), 937–968. doi: 10.1080/00288306.1970.10418211

Gaubert-Boussarie, J., Prado, S., and Hubas, C. (2020). An untargeted metabolomic approach for microphytobenthic biofilms in intertidal mudflats. *Front. Mar. Sci.* 7. doi: 10.3389/fmars.2020.00250

Gavriilidou, A., Gutleben, J., Versluis, D., Forgiarini, F., van Passel, M. W., Ingham, C. J., et al. (2020). Comparative genomic analysis of *Flavobacteriaceae*: insights into carbohydrate metabolism, gliding motility and secondary metabolite biosynthesis. *BMC Genomics* 21 (1), 1–21. doi: 10.1186/s12864-020-06971-7

Gómez-Silva, B., Vilo-Muñoz, C., Galetović, A., Dong, Q., Castelán-Sánchez, H. G., Pérez-Llano, Y., et al. (2019). Metagenomics of Atacama lithobiontic extremophile life unveils highlights on fungal communities, biogeochemical cycles and carbohydrate-active enzymes. *Microorganisms* 7 (12), 619. doi: 10.3390/microorganisms7120619

Gong, B., Cao, H. M., Peng, C. Y., Perculija, V., Tong, G. X., Fang, H. Y., et al. (2019). High-throughput sequencing and analysis of microbial communities in the mangrove swamps along the coast of Beibu Gulf in Guangxi, China. *Sci. Rep.* 9, 9377. doi: 10.1038/s41598-019-45804-w

Guo, B., Wu, X. L., and Qian, Y. (2006). Approaches for increasing the culturability of microorganisms. *Weishengwu Xuebao* 46 (3), 504–507. doi: 10.3321/j.issn:0001-6209.2006.03.036

Harboul, K., Alouiz, I., Hammani, K., and El-Karkouri, A. (2022). Isotherm and kinetics modeling of biosorption and bioreduction of the Cr (VI) by *Brachybacterium paraconglomeratum* ER41. *Extremophiles* 26 (3), 30. doi: 10.1007/s00792-022-01278-9

Hernández-Plaza, A., Szklarczyk, D., Botas, J., Cantalapiedra, C. P., Giner-Lamia, J., Mende, D. R., et al. (2023). eggNOG 6.0: enabling comparative genomics across 12 535 organisms. *Nucleic Acids Res.* 51 (D1), D389–D394. doi: 10.1093/nar/gkac1022

Howard, J., Hoyt, S., Isensee, K., Telszewski, M., and Pidgeon, E. (2014). *Coastal blue carbon: methods for assessing carbon stocks and emissions factors in mangroves, tidal salt marshes, and seagrasses* (Arlington, VA: Conservation International, Intergovernmental Oceanographic Commission of UNESCO, International Union for Conservation of Nature).

Hu, Y. B., Wang, N., Yan, X. C., Yuan, Y., Luo, F., Jiang, Z. Y., et al. (2019). Ginsenoside Re impacts on biotransformation products of ginsenoside Rb1 by Cellulosimicrobium cellulans sp. 21 and its mechanisms. *Process Biochem.* 77, 57–62. doi: 10.1016/j.procbio.2018.11.019

Kanehisa, M., Furumichi, M., Tanabe, M., Sato, Y., and Morishima, K. (2017). KEGG: new perspectives on genomes, pathways, diseases and drugs. *Nucleic Acids Res.* 45 (D1), D353–D361. doi: 10.1093/nar/gkw1092

Kappelmann, L., Krüger, K., Hehemann, J. H., Harder, J., Markert, S., Unfried, F., et al. (2019). Polysaccharide utilization loci of North Sea *Flavobacteriia* as basis for using SusC/D-protein expression for predicting major phytoplankton glycans. *ISME J.* 13 (1), 76–91. doi: 10.1038/s41396-018-0242-6

Katoh, K., and Standley, D. M. (2013). MAFFT multiple sequence alignment software version 7: improvements in performance and usability. *Mol. Biol. Evol.* 30 (4), 772–780. doi: 10.1093/molbev/mst010

Kim, M., Oh, H. S., Park, S. C., and Chun, J. (2014). Towards a taxonomic coherence between average nucleotide identity and 16S rRNA gene sequence similarity for species demarcation of prokaryotes. *Int. J. Systematic Evolutionary Microbiol.* 64 (Pt_2), 346–351. doi: 10.1099/ijs.0.059774-0

Komagata, K., and Suzuki, K. I. (1988). 4 Lipid and cell-wall analysis in bacterial systematics. *Methods Microbiol.* 19, 161–207. doi: 10.1016/S0580-9517(08)70410-0

Konstantinidis, K. T., and Tiedje, J. M. (2005). Towards a genome-based taxonomy for prokaryotes. *J. Bacteriology* 187 (18), 6258–6264. doi: 10.1128/jb.187.18.6258-6264.2005

Krüger, K., Chafee, M., Ben Francis, T., Glavina del Rio, T., Becher, D., Schweder, T., et al. (2019). In marine *Bacteroidetes* the bulk of glycan degradation during algae blooms is mediated by few clades using a restricted set of genes. *ISME J.* 13 (11), 2800–2816. doi: 10.1038/s41396-019-0476-y

Lam-Tung, N., Schmidt, H. A., von Haeseler, A., and Bui Quang, M. (2015). IQ-TREE: A fast and effective stochastic algorithm for estimating maximum-likelihood phylogenies. *Mol. Biol. Evol.* 32 (1), 268–274. doi: 10.1093/molbev/msu300

Lapebie, P., Lombard, V., Drula, E., Terrapon, N., and Henrissat, B. (2019). *Bacteroidetes* use thousands of enzyme combinations to break down glycans. *Nat. Commun.* 10, 2043. doi: 10.1038/s41467-019-10068-5

Lechner, M., Findeiss, S., Steiner, L., Marz, M., Stadler, P. F., and Prohaska, S. J. (2011). Proteinortho: Detection of (Co-)orthologs in large-scale analysis. *BMC Bioinf.* 12, 124. doi: 10.1186/1471-2105-12-124

Li, M. S., Li, T., Zhou, M., Li, M. D., Zhao, Y. X., Xu, J. J., et al. (2021). Caenorhabditis elegans extracts stimulate IAA biosynthesis in *Arthrobacter pascens* ZZ21 *via* the indole-3-pyruvic acid pathway. *Microorganisms* 9 (5), 970. doi: 10.3390/microorganisms9050970

Lichtenthaler, F. W., and Peters, S. (2004). Carbohydrates as green raw materials for the chemical industry. *Comptes Rendus Chimie* 7 (2), 65–90. doi: 10.1016/j.crci.2004.02.002

Liu, Y. L., Meng, D., Li, R. R., Gu, P. F., Fan, X. Y., Huang, Z. S., et al. (2019). *Rhodoligotrophos defluvii* sp. nov., isolated from activated sludge. *Int. J. Systematic Evolutionary Microbiol.* 69 (12), 3830–3836. doi: 10.1099/ijsem.0.003691

Martiny, A. C. (2019). High proportions of bacteria are culturable across major biomes. *ISME J.* 13 (8), 2125–2128. doi: 10.1038/s41396-019-0410-3

Mayor, D. J., Thornton, B., Jenkins, H., and Felgate, S. L. (2018). "Chapter 3 microbiota: the living foundation," in *Mudflat ecology*. Ed. P. G. Beninger (Amsterdam, Netherlands: Springer), 43–61.

McKee, L. S., La Rosa, S. L., Westereng, B., Eijsink, V. G., Pope, P. B., and Larsbrink, J. (2021). Polysaccharide degradation by the *Bacteroidetes*: mechanisms and nomenclature. *Environ. Microbiol. Rep.* 13 (5), 559–581. doi: 10.1111/1758-2229.12980

Meier-Kolthoff, J. P., Carbasse, J. S., Peinado-Olarte, R. L., and Goeker, M. (2022). TYGS and LPSN: a database tandem for fast and reliable genome-based classification and nomenclature of prokaryotes. *Nucleic Acids Res.* 50 (D1), D801–D807. doi: 10.1093/nar/gkab902

Minnikin, D., O'donnell, A., Goodfellow, M., Alderson, G., Athalye, M., Schaal, A., et al. (1984). An integrated procedure for the extraction of bacterial isoprenoid quinones and polar lipids. *J. Microbiological Methods* 2 (5), 233–241. doi: 10.1016/0167-7012(84)90018-6

Mohapatra, M., Yadav, R., Rajput, V., Dharne, M. S., and Rastogi, G. (2021). Metagenomic analysis reveals genetic insights on biogeochemical cycling, xenobiotic degradation, and stress resistance in mudflat microbiome. *J. Environ. Manage.* 292, 112738. doi: 10.1016/j.jenvman.2021.112738

Molari, M., Giovannelli, D., d'Errico, G., and Manini, E. (2012). Factors influencing prokaryotic community structure composition in sub-surface coastal sediments. *Estuarine Coast. Shelf Sci.* 97, 141–148. doi: 10.1016/j.ecss.2011.11.036

Molina-Menor, E., Gimeno-Valero, H., Pascual, J., Peretó, J., and Porcar, M. (2021). High culturable bacterial diversity from a European desert: The Tabernas desert. *Front. Microbiol.* 11. doi: 10.3389/fmicb.2020.583120

Murray, N. J., Phinn, S. R., DeWitt, M., Ferrari, R., Johnston, R., Lyons, M. B., et al. (2019). The global distribution and trajectory of tidal flats. *Nature* 565 (7738), 222–225. doi: 10.1038/s41586-018-0805-8

Nedashkovskaya, O. I., Kim, S. B., Suzuki, M., Shevchenko, L. S., Lee, M. S., Lee, K. H., et al. (2005). *Pontibacter actiniarum* gen. nov., sp nov., a novel member of the phylum *'Bacteroidetes'*, and proposal of *Reichenbachiella* gen. nov as a replacement for the illegitimate prokaryotic generic name *Reichenbachia* Nedashkovskaya et al. 2003. *Int. J. Systematic Evolutionary Microbiol.* 55, 2583–2588. doi: 10.1099/ijs.0.63819-0

Ni, M., Yuan, J. L., Hua, J. Q., Lian, Q. P., Guo, A. H., Liu, M., et al. (2020). Shrimp–vegetable rotational farming system: An innovation of shrimp aquaculture in the tidal flat ponds of Hangzhou Bay, China. *Aquaculture* 518, 734864. doi: 10.1016/j.aquaculture.2019.734864

Pandey, R., Sharma, P., Rathee, S., Singh, H. P., Batish, D. R., Krishnamurthy, B., et al. (2021). Isolation and characterization of a novel hydrocarbonoclastic and biosurfactant producing bacterial strain: *Fictibacillus Phosphorivorans* RP3. *3 Biotech.* 11 (2), 105. doi: 10.1007/s13205-021-02655-5

Park, S., Park, J. M., Lee, K. H., and Yoon, J. H. (2016). *Pontibacter litorisediminis* sp. nov., isolated from a tidal flat. *Int. J. Systematic Evolutionary Microbiol.* 66 (10), 4172–4178. doi: 10.1099/ijsem.0.001331

Parks, D. H., Imelfort, M., Skennerton, C. T., Hugenholtz, P., and Tyson, G. W. (2015). CheckM: assessing the quality of microbial genomes recovered from isolates, single cells, and metagenomes. *Genome Res.* 25 (7), 1043–1055. doi: 10.1101/gr.186072.114

Perillo, G., Wolanski, E., Cahoon, D. R., and Hopkinson, C. S. (2018). *Coastal Wetlands: An Integrated Ecosystem Approach* (Amsterdam: Elsevier).

Rinke, M., Maraun, M., and Scheu, S. (2022). Spatial and temporal variations in salt marsh microorganisms of the Wadden Sea. *Ecol. Evol.* 12 (3), e8767. doi: 10.1002/ece3.8767

Rodriguez-R, L. M., and Konstantinidis, K. T. (2014). Bypassing cultivation to identify bacterial species. *Microbe* 9 (3), 111–118. doi: 10.1128/microbe.9.111.1

Saitou, N., and Nei, M. (1987). The neighbor-joining method: a new method for reconstructing phylogenetic trees. *Mol. Biol. Evol.* 4 (4), 406–425. doi: 10.1093/oxfordjournals.molbev.a040454

Sasmito, S. D., Kuzyakov, Y., Lubis, A. A., Murdiyarso, D., Hutley, L. B., Bachri, S., et al. (2020). Organic carbon burial and sources in soils of coastal mudflat and mangrove ecosystems. *Catena* 187, 104414. doi: 10.1016/j.catena.2019.104414

Sasser, M. (1990). *Identification of bacteria by gas chromatography of cellular fatty acids* (Newark, DE: Microbial ID Inc). Available at: http://www.microbialid.com/PDF/TechNote_101.pdf.

Schroeter, R., Voigt, B., Jürgen, B., Methling, K., Pöther, D. C., Schäfer, H., et al. (2011). The peroxide stress response of *Bacillus licheniformis*. *Proteomics* 11 (14), 2851–2866. doi: 10.1002/pmic.201000461

Seemann, T. (2014). Prokka: rapid prokaryotic genome annotation. *Bioinformatics* 30 (14), 2068–2069. doi: 10.1093/bioinformatics/btu153

Sefrji, F. O., Marasco, R., Michoud, G., Seferji, K. A., Merlino, G., and Daffonchio, D. (2022). Insights Into the Cultivable Bacterial Fraction of Sediments From the Red Sea Mangroves and Physiological, Chemotaxonomic, and Genomic Characterization of *Mangrovibacillus cuniculi* gen. nov., sp. nov., a Novel Member of the *Bacillaceae* Family. *Front. Microbiol.* 13. doi: 10.3389/fmicb.2022.777986

Sefrji, F. O., Michoud, G., Marasco, R., Merlino, G., and Daffonchio, D. (2021). *Mangrovivirga cuniculi* gen. nov., sp. nov., a moderately halophilic bacterium isolated from bioturbated Red Sea mangrove sediment, and proposal of the novel family *Mangrovivirgaceae* fam. nov. *Int. J. Systematic Evolutionary Microbiol.* 71 (7), 4866. doi: 10.1099/ijsem.0.004866

Shi, X. L., Wu, Y. H., Jin, X. B., Wang, C. S., and Xu, X. W. (2017). *Alteromonas lipolytica* sp. nov., a poly-beta-hydroxybutyrate-producing bacterium isolated from surface seawater. *Int. J. Systematic Evolutionary Microbiol.* 67 (2), 237–242. doi: 10.1099/ijsem.0.001604

Siamphan, C., Chang, Y. H., and Kim, W. (2015). *Eudoraea chungangensis* sp nov., isolated from an aquafarm waste water sludge. *Antonie Van Leeuwenhoek Int. J. Gen. Mol. Microbiol.* 107 (4), 1009–1015. doi: 10.1007/s10482-015-0393-7

Staloch, B. E. K., Niero, H., de Freitas, R. C., Ballone, P., Rodrigues-Costa, F., Trivella, D. B. B., et al. (2022). Draft genome sequence of *Psychrobacter nivimaris* LAMA 639 and its biotechnological potential. *Data Brief* 41, 107927. doi: 10.1016/j.dib.2022.107927

Steen, A. D., Crits-Christoph, A., Carini, P., DeAngelis, K. M., Fierer, N., Lloyd, K. G., et al. (2019). High proportions of bacteria and archaea across most biomes remain uncultured. *ISME J.* 13 (12), 3126–3130. doi: 10.1038/s41396-019-0484-y

Subhash, Y., Tushar, L., Sasikala, C., and Ramana, C. V. (2013). *Erythrobacter odishensis* sp nov and *Pontibacter odishensis* sp nov isolated from dry soil of a solar saltern. *Int. J. Systematic Evolutionary Microbiol.* 63, 4524–4532. doi: 10.1099/ijs.0.052183-0

Tamura, K., Stecher, G., and Kumar, S. (2021). MEGA11 molecular evolutionary genetics analysis version 11. *Mol. Biol. Evol.* 38 (7), 3022–3027. doi: 10.1093/molbev/msab120

Tang, K., Lin, Y., Han, Y., and Jiao, N. (2017). Characterization of potential polysaccharide utilization systems in the marine bacteroidetes gramella flava JLT2011 using a multi-omics approach. *Front. Microbiol.* 8. doi: 10.3389/fmicb.2017.00220

Terrapon, N., Lombard, V., Drula, E., Lapebie, P., Al-Masaudi, S., Gilbert, H. J., et al. (2018). PULDB: the expanded database of Polysaccharide Utilization Loci. *Nucleic Acids Res.* 46 (D1), D677–D683. doi: 10.1093/nar/gkx1022

Terrapon, N., Lombard, V., Gilbert, H. J., and Henrissat, B. (2015). Automatic prediction of polysaccharide utilization loci in *Bacteroidetes* species. *Bioinformatics* 31 (5), 647–655. doi: 10.1093/bioinformatics/btu716

Tindall, B. J., Rosselló-Móra, R., Busse, H. J., Ludwig, W., and Kämpfer, P. (2010). Notes on the characterization of prokaryote strains for taxonomic purposes. *Int. J. Systematic Evolutionary Microbiol.* 60 (1), 249–266. doi: 10.1099/ijs.0.016949-0

Torsvik, V., and Ovreas, L. (2002). Microbial diversity and function in soil: from genes to ecosystems. *Curr. Opin. Microbiol.* 5 (3), 240–245. doi: 10.1016/s1369-5274(02)00324-7

Underwood, G. J. C., and Kromkamp, J. (1999). Primary production by phytoplankton and microphytobenthos in estuaries. *Adv. Ecol. Res.* 29, 93–153. doi: 10.1016/s0065-2504(08)60192-0

Unfried, F., Becker, S., Robb, C. S., Hehemann, J.-H., Markert, S., Heiden, S. E., et al. (2018). Adaptive mechanisms that provide competitive advantages to marine bacteroidetes during microalgal blooms. *ISME J.* 12 (12), 2894–2906. doi: 10.1038/s41396-018-0243-5

Wang, Y., Nie, M. Q., Diwu, Z. J., Chang, F., Nie, H. Y., Zhang, B., et al. (2021). Toxicity evaluation of the metabolites derived from the degradation of phenanthrene by one of a soil ubiquitous PAHs-degrading strain *Rhodococcus qingshengii* FF. *J. Hazardous Materials* 415, 125657. doi: 10.1016/j.jhazmat.2021.125657

Wang, X. X., Xiao, X. M., Zou, Z. H., Chen, B. Q., Ma, J., Dong, J. W., et al. (2020b). Tracking annual changes of coastal tidal flats in China during 1986–2016 through analyses of Landsat images with Google Earth Engine. *Remote Sens. Environ.* 238, 110987. doi: 10.1016/j.rse.2018.11.030

Wang, G. H., Xu, S. L., Dang, G., Liu, J. F., Su, H. F., Chen, B. A., et al. (2020a). *Poritiphilus flavus* gen. nov., sp. nov., a member of the family Flavobacteriaceae isolated from coral Porites lutea. *Int. J. Systematic Evolutionary Microbiol.* 70 (11), 5620–5626. doi: 10.1099/ijsem.0.004452

Williams, S., and Davies, F. (1965). Use of antibiotics for selective isolation and enumeration of actinomycetes in soil. *Microbiology* 38 (2), 251–261. doi: 10.1099/00221287-38-2-251

Xu, J., Bjursell, M. K., Himrod, J., Deng, S., Carmichael, L. K., Chiang, H. C., et al. (2003). A genomic view of the human-*Bacteroides* thetaiotaomicron symbiosis. *Science* 299 (5615), 2074–2076. doi: 10.1126/science.1080029

Xu, L., Wu, Y. H., Zhou, P., Cheng, H., Liu, Q., and Xu, X. W. (2018). Investigation of the thermophilic mechanism in the genus *Porphyrobacter* by comparative genomic analysis. *BMC Genomics* 19, 385. doi: 10.1186/s12864-018-4789-4

Yoon, S. H., Ha, S. M., Lim, J., Kwon, S., and Chun, J. (2017). A large-scale evaluation of algorithms to calculate average nucleotide identity. *Antonie Van Leeuwenhoek Int. J. Gen. Mol. Microbiol.* 110 (10), 1281–1286. doi: 10.1007/s10482-017-0844-4

Yuan, H. L., Xu, Y., Chen, Y. Z., Zhan, Y. Y., Wei, X. T., Li, L., et al. (2019). Metabolomics analysis reveals global acetoin stress response of *Bacillus licheniformis*. *Metabolomics* 15, 1–12. doi: 10.1007/s11306-019-1492-7

Zhang, R., Sun, M. R., Zhang, H. L., and Zhao, Z. H. (2021). Spatial separation of microbial communities reflects gradients of salinity and temperature in offshore sediments from Shenzhen, south China. *Ocean Coast. Manage.* 214, 105904. doi: 10.1016/j.ocecoaman.2021.105904

Zhang, H., Yohe, T., Huang, L., Entwistle, S., Wu, P. Z., Yang, Z. L., et al. (2018). dbCAN2: a meta server for automated carbohydrate-active enzyme annotation. *Nucleic Acids Res.* 46 (W1), W95–W101. doi: 10.1093/nar/gky418

Zhang, L., Zhang, Q. J., Luo, X. S., Tang, Y. L., Dai, J., Li, Y. W., et al. (2008). *Pontibacter korlensis* sp nov., isolated from the desert of Xinjiang, China. *Int. J. Systematic Evolutionary Microbiol.* 58, 1210–1214. doi: 10.1099/ijs.0.65667-0

Zheng, Z. G., Zheng, J. S., Liu, H. L., Peng, D. H., and Sun, M. (2016). Complete genome sequence of Fictibacillus phosphorivorans G25-29, a strain toxic to nematodes. *J. Biotechnol.* 239, 20–22. doi: 10.1016/j.jbiotec.2016.09.014

Zou, H. Y., Berglund, B., Xu, H., Chi, X. H., Zhao, Q., Zhou, Z. Y., et al. (2020). Genetic characterization and virulence of a carbapenem-resistant *Raoultella ornithinolytica* isolated from well water carrying a novel megaplasmid containing bla (NDM-1). *Environ. pollut.* 260, 114041. doi: 10.1016/j.envpol.2020.114041